Microsolvation of the Dicyanamide Anion: $[N(CN)_2^-](H_2O)_n$ ($n = 0-12$)

Barbara Jagoda-Cwiklik,[†] Xue-Bin Wang,[‡] Hin-Koon Woo,[‡] Jie Yang,[‡] Guan-Jun Wang,[§] Mingfei Zhou,*[,§] Pavel Jungwirth,*[,†] and Lai-Sheng Wang*[,‡]

Institute of Organic Chemistry and Biochemistry, Academy of Sciences of the Czech Republic, and Center for Biomolecules and Complex Molecular Systems, Flemingovo nám. 2, 16610 Prague 6, Czech Republic, Department of Physics, Washington State University, 2710 University Drive, Richland, Washington 99354, Chemical Science Division, Pacific Northwest National Laboratory, MS K8-88, P. O. Box 999, Richland, Washington 99352, and Department of Chemistry & Laser Chemistry Institute, Shanghai Key Laboratory of Molecular Catalysis and Innovative Materials, Fudan University, Shanghai 200433, China

Received: March 6, 2007; In Final Form: June 1, 2007

Photoelectron spectroscopy is combined with ab initio calculations to study the microsolvation of the dicyanamide anion, $N(CN)_2^-$. Photoelectron spectra of $[N(CN)_2^-](H_2O)_n$ ($n = 0-12$) have been measured at room temperature and also at low temperature for $n = 0-4$. Vibrationally resolved photoelectron spectra are obtained for $N(CN)_2^-$, allowing the electron affinity of the $N(CN)_2$ radical to be determined accurately as 4.135 ± 0.010 eV. The electron binding energies and the spectral width of the hydrated clusters are observed to increase with the number of water molecules. The first five waters are observed to provide significant stabilization to the solute, whereas the stabilization becomes weaker for $n > 5$. The spectral width, which carries information about the solvent reorganization upon electron detachment in $[N(CN)_2^-](H_2O)_n$, levels off for $n > 6$. Theoretical calculations reveal several close-lying isomers for $n = 1$ and 2 due to the fact that the $N(CN)_2^-$ anion possesses three almost equivalent hydration sites. In all the hydrated clusters, the most stable structures consist of a water cluster solvating one end of the $N(CN)_2^-$ anion.

1. Introduction

First synthesized in 1925,[1] the dicyanamide anion $N(CN)_2^-$ and particularly its transition metal salts have recently attracted considerable attention,[2−7] because of their potential use as molecular magnets and multifunctional materials. The structures and properties of many dicyanamide salts have been characterized by a variety of spectroscopic techniques.[3−5,8,9] Bare $N(CN)_2^-$ anion is a prototype of a class of five-atom, 24-valence electron chainlike molecules,[10,11] and its high stability has inspired theoretical searches for other isoelectronic species, such as N_5^+ and $OCNCO^+$.[12−14] Organic salts of $N(CN)_2^-$ have recently been discovered to be low-viscosity room-temperature ionic liquids.[15] Vibrational spectroscopy and dynamics of $N(CN)_2^-$ in solution have been carried out to elucidate the interactions of $N(CN)_2^-$ with different solvents,[16] as well as simulations by molecular force field.[17]

Photoelectron spectroscopy (PES) of solvated cluster anions is a powerful experimental technique to probe the molecular interactions between solute and solvent.[18−20] It provides electronic structure information, as well as sequential solvation energies one solvent molecule at a time. Ab initio calculations provide complementary structural and energetic information, which can be directly compared with the PES data. Using an electrospray ionization (ESI) source and PES, we have produced and investigated a variety of complex anions solvated by water, including a series of dicarboxylate dianions,[21,22] the sulfate dianion (SO_4^{2-}),[23,24] the sodium sulfate ion pair,[25] nitrate (NO_3^-),[26] and azide (N_3^-) anions.[27]

In the present article, we report a combined PES and ab initio study on the microsolvation of the dicyanamide anion, $[N(CN)_2^-](H_2O)_n$ ($n = 0-12$).

2. Experimental and Theoretical Methods

2.1. Photoelectron Spectroscopy. The experiments were performed with two home-built apparatuses that couple an ESI source to a magnetic-bottle time-of-flight photoelectron spectrometer. The solvated clusters, $N(CN)_2^-(H_2O)_n$ ($n = 0-12$), were generated via electrospray of 1 mM $NaN(CN)_2$ solution in a water/methanol mixed solvent. Room-temperature experiments were carried out on an ESI-PES instrument that has been described in detail elsewhere.[28] For smaller $N(CN)_2^-(H_2O)_n$ clusters with $n = 0-4$, we also obtained PES data using a newly developed instrument that has the ability to cool ions to low temperatures.[29,30] In this case, the anions produced from the ESI source were guided by two rf-only devices and a 90° ion bender into a Paul trap, which is attached to the cold head of a cryostat (10−400 K). In the current experiment, the ion trap was operated at 68 K and ions were collisionally cooled by ~1 mTorr of N_2 background gas for 0.1 s before pulsed out into the extraction zone of a time-of-flight mass spectrometer.

During each PES experiment, anions of interest were mass selected and decelerated before being intercepted by a detachment laser beam in the interaction zone of a magnetic-bottle photoelectron analyzer. The spectra of the bare $N(CN)_2^-$ anion were obtained at both 266 nm (4.661 eV) and 193 nm (6.424 eV), while the clusters were only taken at 193 nm. Photoelectrons were collected with high efficiency using the magnetic-

* Corresponding authors. E-mail: mfzhou@fudan.edu.cn (M.Z.); pavel.jungwirth@uochb.cas.cz (P.J.); ls.wang@pnl.gov (L.S.W.).

[†] Academy of Sciences of the Czech Republic and Center for Biomolecules and Complex Molecular Systems.

[‡] Washington State University and Pacific Northwest National Laboratory.

[§] Fudan University.

10.1021/jp071832n CCC: $37.00
Published on Web 07/20/2007

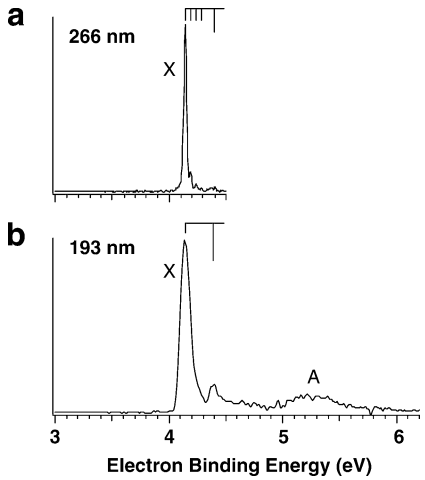

Figure 1. Low-temperature photoelectron spectra of $N(CN)_2^-$ at (a) 266 and (b) 193 nm.

bottle-type electron analyzers.[28−30] Photoelectron time-of-flight spectra were collected and then converted into kinetic energy spectra, calibrated by the known spectra of I^- and ClO_2^-. Electron binding energy spectra were obtained by subtracting the kinetic energy spectra from the detachment photon energies, followed by a constant energy smoothing procedure (5 meV for 266 nm, 10 meV for 193 nm). The energy resolution ($\Delta E/E$) was estimated to be approximately 2%, i.e., approximately 20 meV for 1 eV electrons.

2.2. Theoretical Methods. We performed ab initio calculations for $[N(CN)_2^-](H_2O)_n$ clusters ($n = 0-6$) in order to obtain molecular structure information and understand the nature of interactions between water molecules and the dicyanamide anion. Geometries were optimized and vertical detachment energies (VDEs) were evaluated at the MP2/aug-cc-pvdz level of theory using the Gaussian 03 program package.[31] For each of the $[N(CN)_2^-](H_2O)_n$ clusters we did geometry optimizations starting from various chemically plausible structures with no symmetry constraints. Frequency analysis was done to verify that the optimized structures correspond to minima on the potential energy surface. The VDE was calculated as the difference between the energy of the optimized anionic structure and that of the corresponding neutral at the anionic geometry. ROMP2 energies were used for open-shell neutrals. For clusters with up to four water molecules we were also able to calculate the VDEs at the CCSD(T)/aug-cc-pvdz level. For the global minimum of each cluster we calculated the "vertical" sequential binding or solvation energy of the water molecules. This quantity was evaluated as the energy of the optimized $[N(CN)_2^-](H_2O)_n$ cluster minus the energies of a water molecule and a $[N(CN)_2^-](H_2O)_{n-1}$ cluster without additional geometry changes. These water binding energies were corrected for the basis set superposition error using a standard counterpoise scheme.[32]

3. Experimental Results

3.1. $N(CN)_2^-$. Figure 1 shows the low-temperature PES spectra of the bare $N(CN)_2^-$ anion at 266 and 193 nm. The 193 nm spectrum (Figure 1b) reveals an intense ground-state transition (X) and a very broad band (A) centered at 5.2−5.3 eV, which should correspond to the first excited state of the $N(CN)_2$ radical. A short vibrational progression was observed in the X band with a vibrational spacing of 2100 cm^{-1}. At 266 nm (Figure 1a), a low-frequency mode was further resolved with an average spacing of 400 cm^{-1}. The full width at half-maximum of the 0−0 transition is 20 meV, very close to the instrumental resolution. The well-resolved 0−0 transition yields an accurate adiabatic detachment energy (ADE) for $N(CN)_2^-$ as 4.135 ± 0.010 eV, which also represents the electron affinity (EA) of the $N(CN)_2$ radical.

3.2. $N(CN)_2^-(H_2O)_n$. The room-temperature spectra of the hydrated clusters $[N(CN)_2^-](H_2O)_n$ ($n = 1-12$) at 193 nm are presented in Figure 2, in comparison with that of the bare $N(CN)_2^-$ anion. The spectra of the solvated clusters are similar to those of the bare anion, except for a gradual increase in the electron binding energies and broadening of the spectral features with increasing n. For small clusters ($n = 1-3$), both the X and A bands are observed, whereas for $n = 4-10$, only the X band and the onset of the A band are observed. For $n > 10$, even the X band is partially cut off due to the increased electron binding energies as a result of the solvation stabilization to the anions. The increased spectral width for the hydrated clusters is owing to the expected large anion−neutral geometry changes upon electron detachment and may also be related to the coexistence of multiple low-lying isomers (see below).

3.3. Adiabatic and Vertical Detachment Energies. The ADEs and VDEs for $[N(CN)_2^-](H_2O)_n$ ($n = 0-12$) are listed in Table 1. For $N(CN)_2^-$, the ADE and VDE are identical because the geometry change between the anion and neutral is negligible. For the solvated clusters, the spectra become broader due to solvent relaxation upon electron detachment. Because vibrational features were no longer resolved, the ADEs for each solvated species were estimated by drawing a straight line at the leading edge of the respective X bands and then adding a constant to the intercept with the binding energy axis to take into account both the instrumental resolution and a finite thermal effect for the room-temperature spectra, and only the former for the cold spectra due to removal of vibrational hot bands. The instrumental resolution is dependent on the electron kinetic energy, so is the corrected constant. The typical corrected constant for electrons with 1.5 eV kinetic energy is ∼50 meV for the resolution and ∼150 meV for both the resolution and thermal effect. The VDEs were measured from the X peak maxima in each spectrum. The listed ADEs and VDEs for $n = 0-4$ are from the low-temperature spectra (see below). Both ADEs and VDEs are observed to increase monotonically with the number of solvated water molecules (Table 1 and Figure 3).

3.4. Comparison of Room-Temperature and Low-Temperature Spectra. Figure 4 shows the low-temperature spectra of $N(CN)_2^-(H_2O)_n$ ($n = 0-4$) at 193 nm (blue), compared to those taken at room temperature (red). A substantial blue shift in the threshold in the low-temperature spectra is observed by about 80, 100, 100, and 50 meV for $n = 0$, 1, 2, and 3, respectively. The peak maximum (VDE) of $n = 1$ and 2 are also found to shift to higher binding energies by about 20 and 30 meV. The threshold blue shift and sharper onset in the low-temperature spectra are due to the elimination of hot bands at low temperatures or possibly reduction of anion isomers. However, we did not observe significant changes in the low-temperature spectrum for $n = 4$. No low-temperature spectra were taken for larger clusters due to weaker mass signals and the difficulty of observing significant spectral improvements.

4. Theoretical Results

4.1. $N(CN)_2^-(H_2O)$ and $N(CN)_2^-(H_2O)_2$. The optimized structure of the bare $N(CN)_2^-$ anion is planar with C_{2v} symmetry (Figure 5a). Adding the first water molecule breaks the symmetry of the anion with water preferentially binding to one of the terminal nitrogen atoms (Figure 5b). The N···H hydrogen bond distance is 1.87 Å with a solvation energy of 11.4 kcal/

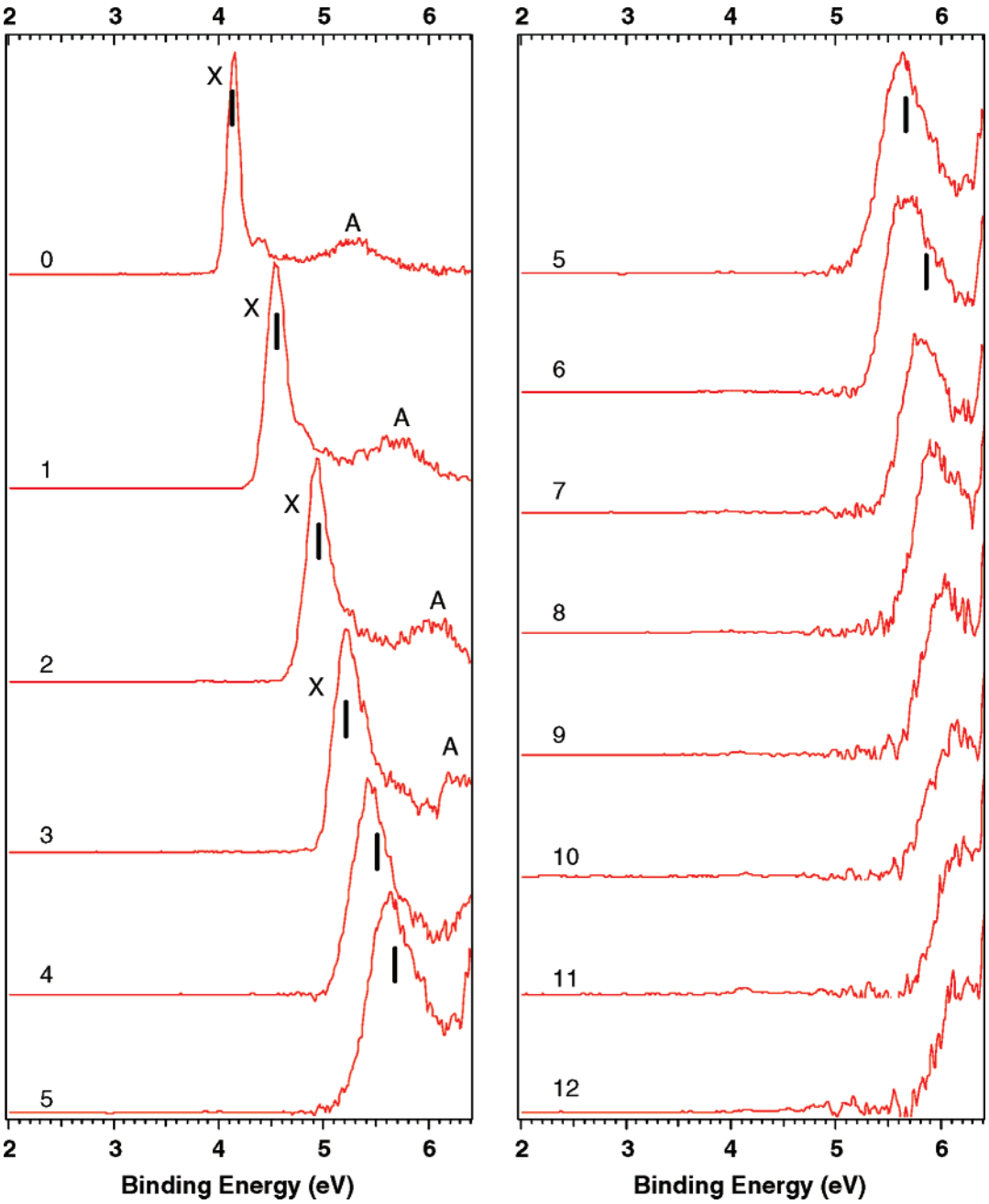

Figure 2. Room-temperature photoelectron spectra of $N(CN)_2^-(H_2O)_n$ ($n = 0-12$) at 193 nm. The vertical bars represent the calculated vertical detachment energies for the lowest energy structures for $n = 0-6$ at MP2/aug-cc-pvdz level.

mol (Table 2). We also found a second structure with water bound to the central nitrogen (Figure 5c), which lies only 0.7 kcal/mol above the global minimum. The N···H hydrogen bond distance in this case amounts to 1.95 Å.

The four lowest structures of the $[N(CN)_2^-](H_2O)_2$ cluster are depicted in Figure 5d−g. Three of these structures lie within 0.50 kcal/mol, and the fourth is less than 3 kcal/mol higher in energy. In the lowest energy structure (Figure 5d), each of the two water molecules is bound to a different nitrogen atom, while they form an additional water−water H-bond. For the global minimum, the H-bond lengths with the terminal and the central nitrogen atoms are 1.84 and 2.23 Å, respectively, while the H-bond length between the two water molecules is 2.02 Å. The solvation energies are slightly larger than in the $n = 1$ cluster, amounting to 12.1 and 12.2 kcal/mol.

It is noteworthy that for $n = 1$ and 2 there are several low-lying structures with very close energies. This unusual situation is due to the presence of three hydrogen bond acceptors in $N(CN)_2^-$ with similar water affinity (the charge distributions on the two terminal and the central N atoms are −0.3, −0.3, and −0.4, respectively).[11]

4.2. $N(CN)_2^-(H_2O)_3$ and $N(CN)_2^-(H_2O)_4$. The $[N(CN)_2^-](H_2O)_3$ cluster behaves similarly to the $n = 2$ case in the sense that H-bonds between water molecules enhance the solvation energy and such structures are preferred. The geometry with a three-water ring (Figure 5h) is the global minimum and is favored by almost 3 kcal/mol over those possessing two or only one water−water H-bond. The H-bond distances between nitrogen and hydrogen atoms for the lowest structure are 2.02, 2.14, and 2.21 Å. The corresponding water solvation energies increase again in comparison with the $[N(CN)_2^-](H_2O)_2$ cluster, amounting to 13.3, 13.9, and 15.1 kcal/mol.

For $n = 4$, four low-lying optimized structures were found (Figure 5k−n). The lowest structure is similar to that in

TABLE 1: Experimental Adiabatic (ADE) and Vertical (VDE) Detachment Energies (eV) for $N(CN)_2^-(H_2O)_n$ ($n = 0-12$) Compared with the Calculated VDEs at Two Levels of Theory

n	ADE_{expt}[a]	VDE_{expt}	VDE_{MP2}[b]	$VDE_{CCSD(T)}$[c]
0	4.135 ± 0.010	4.135 ± 0.010	4.11	3.99
1	4.50 ± 0.02	4.54 ± 0.02	4.55, 4.60	4.44, 4.49
2	4.88 ± 0.02	4.95 ± 0.02	4.96, 4.98, 4.91, 5.09	4.86, 4.86, 4.81, 4.99
3	5.12 ± 0.02	5.22 ± 0.02	5.21, 5.37, 5.36	5.00
4	5.22 ± 0.05	5.38 ± 0.05	5.51, 5.91, 5.44, 5.67	5.41
5	5.38 ± 0.10	5.61 ± 0.10	5.68	
6	5.42 ± 0.10	5.66 ± 0.10	5.88	
7	5.58 ± 0.10	5.80 ± 0.10		
8	5.72 ± 0.10	5.91 ± 0.10		
9	5.80 ± 0.10	6.02 ± 0.10		
10	5.85 ± 0.10	6.14 ± 0.10		
11	5.95 ± 0.10	6.20 ± 0.10		
12	5.98 ± 0.10	6.24 ± 0.10		

[a] Also represents the electron affinity (EA) of the corresponding neutral. [b] At MP2/aug-cc-pvdz level. For $n = 1-4$, the VDEs for all geometries in Figure 3, while for $n = 5$ and 6 only the lowest energy structures are calculated. [c] At the CCSD(T)/aug-cc-pvdz level. The VDEs are calculated for all geometries for $n = 1$, 2 and only for the global minima for $n = 3$, 4.

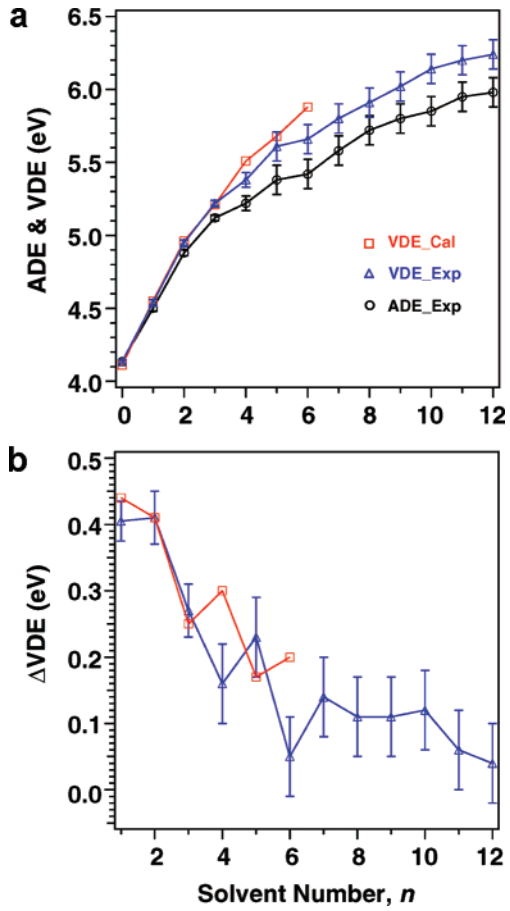

Figure 3. (a) Adiabatic (ADE) and vertical (VDE) detachment energies of $N(CN)_2^-(H_2O)_n$ as a function of solvent number n. (b) Incremental electron stabilization energies, $\Delta VDE = VDE(n) - VDE(n-1)$, as a function of solvent number (n).

$[N(CN)_2^-](H_2O)_3$ with the solvation ring extended from three to four water molecules. The other three structures, which are significantly higher in energy, possess either smaller, three-water rings (Figure 5l,m) or a water chain (Figure 5n). For the lowest structure, the N···H hydrogen bond distances are equal to 2.24 Å for the central N atom, and 2.32 and 2.34 Å for the terminal nitrogen. The water solvation energies for this structure rise to approximately 15.5 kcal/mol each. We stress that for the energetically low-lying clusters with $n = 1-4$ all water molecules are bound directly to the nitrogen atoms of the anion.

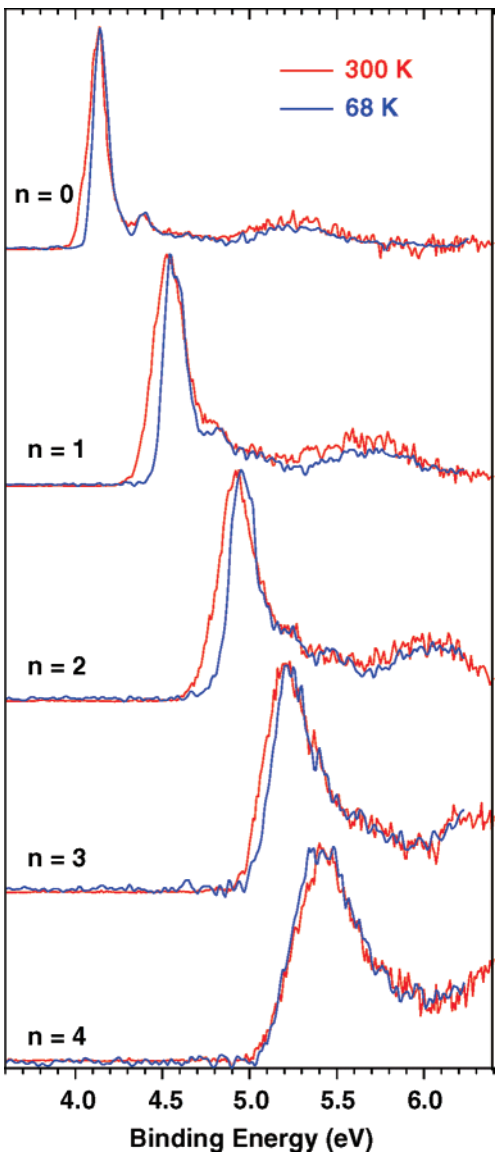

Figure 4. Comparison of low-temperature (blue) and room-temperature (red) photoelectron spectra of $N(CN)_2^-(H_2O)_n$ ($n = 0-4$) at 193 nm.

4.3. $N(CN)_2^-(H_2O)_5$ and $N(CN)_2^-(H_2O)_6$. The binding pattern of water molecules changes in the cases of $n = 5$ and 6 (Figure 6). In the lowest energy structures in both cases, a cluster of water molecules is formed where one or two water molecules are not directly bound to nitrogen but are rather

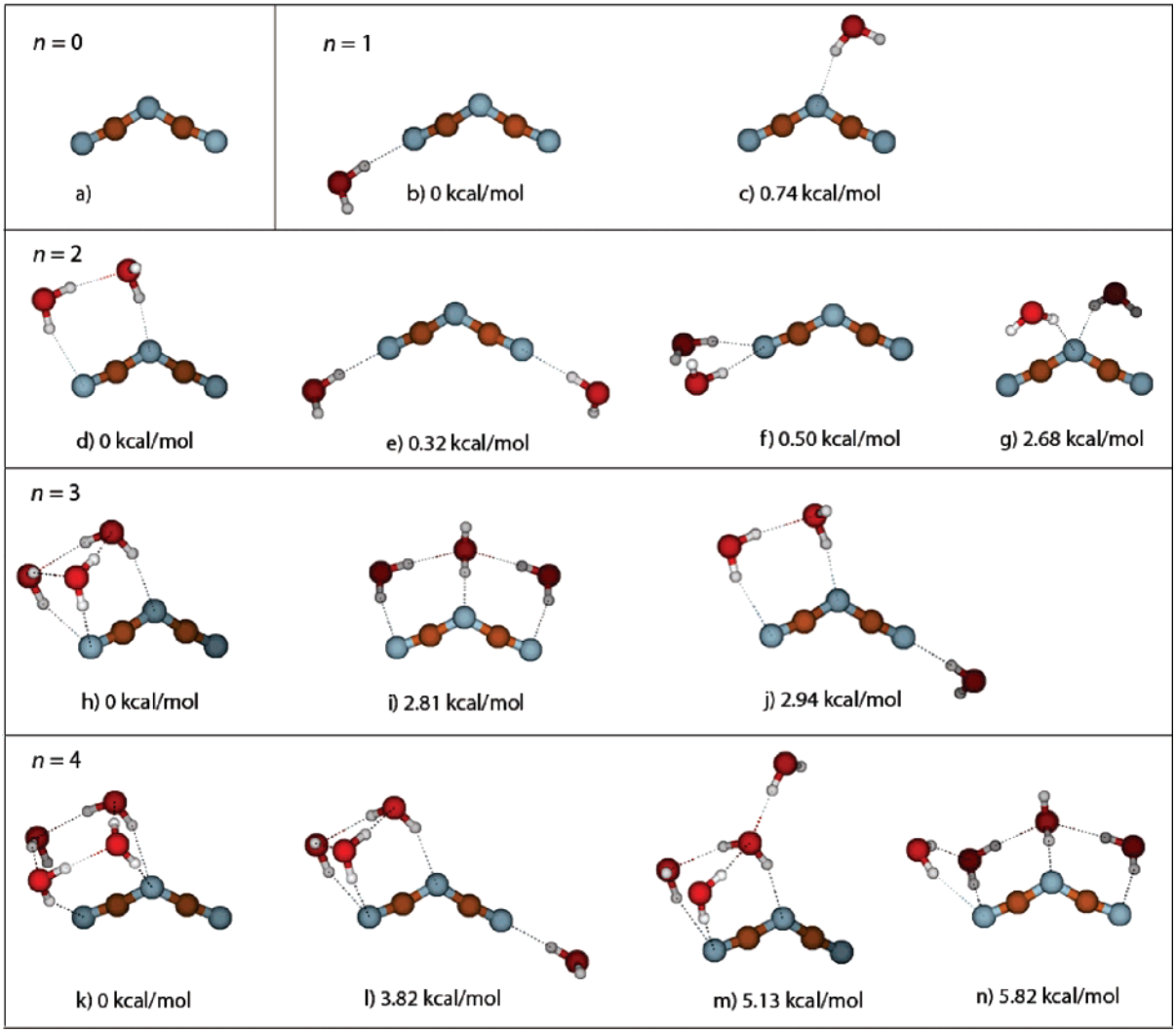

Figure 5. Structures and energetics of $N(CN)_2^-(H_2O)_n$ for $n = 0-4$.

TABLE 2: Calculated Vertical Solvation Energies of Individual Water Molecules and the N···H H-Bond Distances for the Lowest Energy Structures of $N(CN)_2^-(H_2O)_n$ ($n = 1-6$)

n	$E_{binding}$ (kcal/mol)	$R_{N\cdots H}$ (Å)
1	11.40	1.87
2	12.10, 12.25	1.84, 2.23
3	13.32, 13.93, 15.06	2.02, 2.14, 2.21
4	15.32, 15.55, 15.57, 15.60	2.24, 2.24, 2.32, 2.34
5	11.71, 15.02, 15.72, 16.90, 17.72	1.86, 2.14, 2.20, 2.20
6	13.67, 14.26, 16.44, 16.46, 17.51, 18.62	1.83, 2.12, 2.13, 2.14

located in a second solvation shell, forming H-bonds only with other water molecules. The water molecules from the second solvation shell are more weakly bound by about 3−5 kcal/mol compared to water molecules in the first solvation shell (Table 2). Also note that for the $[N(CN)_2^-](H_2O)_n$ solvated clusters with n up to 6 a water cluster at one side of the anion is energetically preferred over a more even solvent distribution. Only for larger clusters, perhaps, can one expect the formation of a more symmetric and interconnected water structure for the global minimum.

5. Discussion

5.1. Photoelectron Spectra of $N(CN)_2^-$. The sharp, dominant 0−0 transition revealed in the PES spectra of $N(CN)_2^-$ (Figure 1) indicates that there is little geometrical change between the anion and the neutral $N(CN)_2$ radial. Indeed, our calculation shows that the optimal structure of the $N(CN)_2$ radical has almost identical bond lengths and angles compared to that of the anion. The only observable changes are the bond lengths of the terminal N−C bonds, which shorten by 0.04 Å, and the N−C−N bond angle, which increases by 1.3°. Therefore, the two observed vibrational modes should correspond to the terminal N−C stretching (2100 cm^{-1}) and the N−C−N bending (400 cm^{-1}) modes, respectively, consistent with the assignments based on the bulk measurements.[3,4,11] This geometry rigidity and the spectrum can be qualitatively explained by examining the highest occupied molecular orbital (HOMO) of $N(CN)_2^-$. As shown in Figure 7, the HOMO of $N(CN)_2^-$ is a weakly antibonding π orbital primarily from the three N atoms. The slight geometry changes from the anion to the neutral ground state are consistent with the nature of the HOMO. The calculated VDE from detaching an electron from the HOMO is 4.11 eV, in excellent agreement with the experimental result.

Detaching one electron from the next HOMO−1 gives rise to the A band in the 193 nm spectrum (Figure 1b). As indicated in Figure 7, the HOMO−1 involves strong terminal C−N bonding character and bonding interactions between the two terminal CN groups. Thus removal of an electron from HOMO−1 is expected to induce large increases in the terminal C−N bonds and the large N−C−N bond angle changes, consistent with the broad A band in Figure 1b. The energy

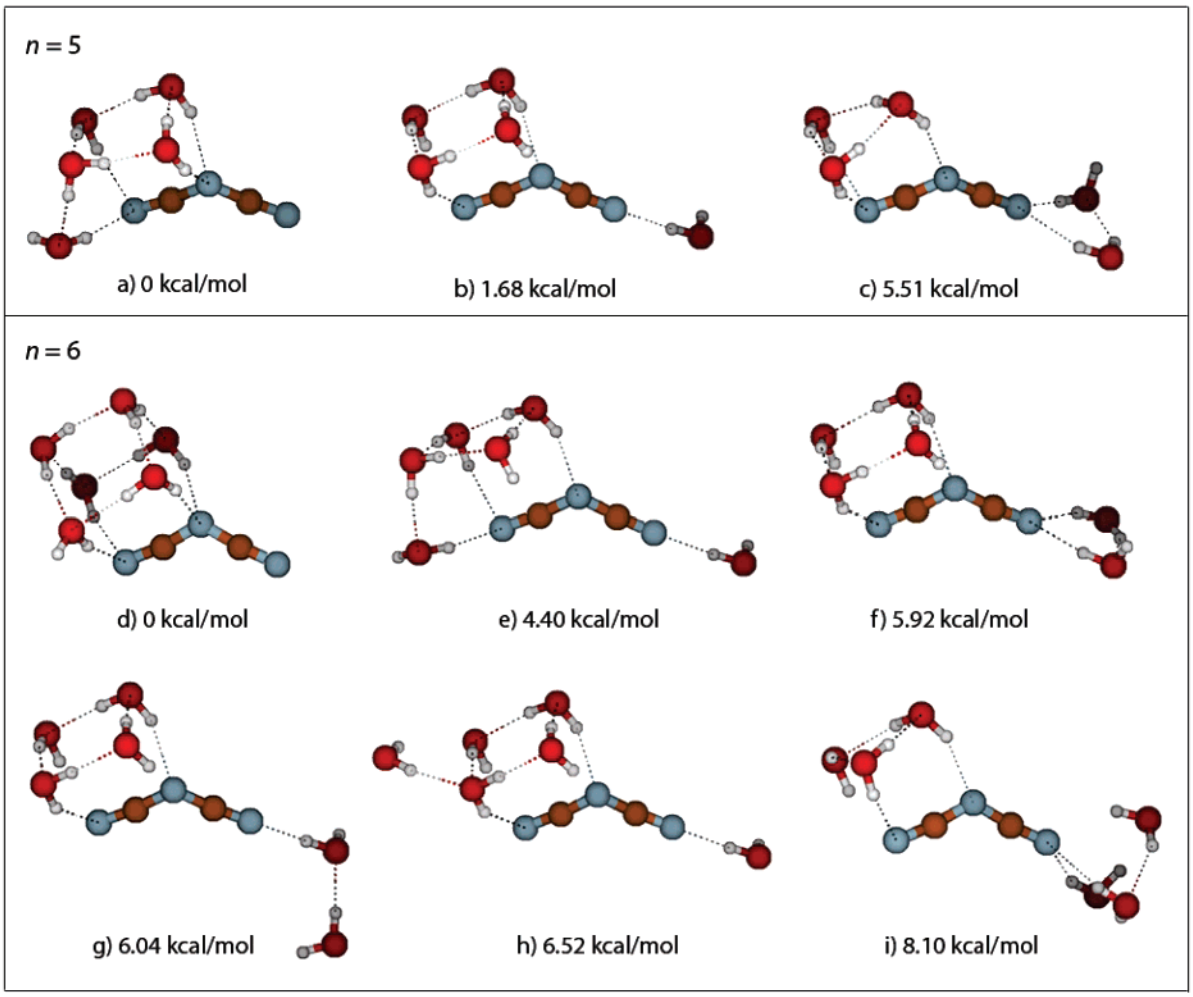

Figure 6. Structures and energetics of $N(CN)_2^-(H_2O)_n$ for $n = 5$ and 6.

difference of 1.26 eV between HOMO and HOMO−1 also agrees with the energy separation between the X and A bands.

5.2. Spectral Width and Solvent Reorganization. The single vibrational transition of the ground state, as well as the well-separated excited-state feature in the $N(CN)_2^-$ spectrum, makes it possible to examine the spectral broadening induced by solvation in $N(CN)_2^-(H_2O)_n$. As shown in Figure 2, the width of the X peak gradually increases with the solvent number from $n = 0$ to 5, and stays roughly constant for $n \geq 6$. The nature of this width is a result of the Franck−Condon overlap from the ground state of the anion to the ground state of the corresponding neutral clusters, reflecting the structural change (reorganization) of the clusters upon electron detachment. Because of the negligible geometry changes for the solute $N(CN)_2^-$, the width of the X peaks in Figure 2 should be entirely due to the reorganization of the water molecules around the solute upon electron detachment. The H-bonding strength between the solute and solvent changes dramatically upon electron detachment, leading to large (solvation) structural changes that are reflected in the PES bandwidth. The roughly constant width for $n \geq 6$ is consistent with the theoretical results in Figure 6, which shows that additional waters do not bond directly to the solute anion, thus making negligible contributions to the solvent reorganization energies.

5.3. Electron Binding Energy and Microsolvation. The calculated VDEs of $[N(CN)_2^-](H_2O)_n$ for all low-lying structures

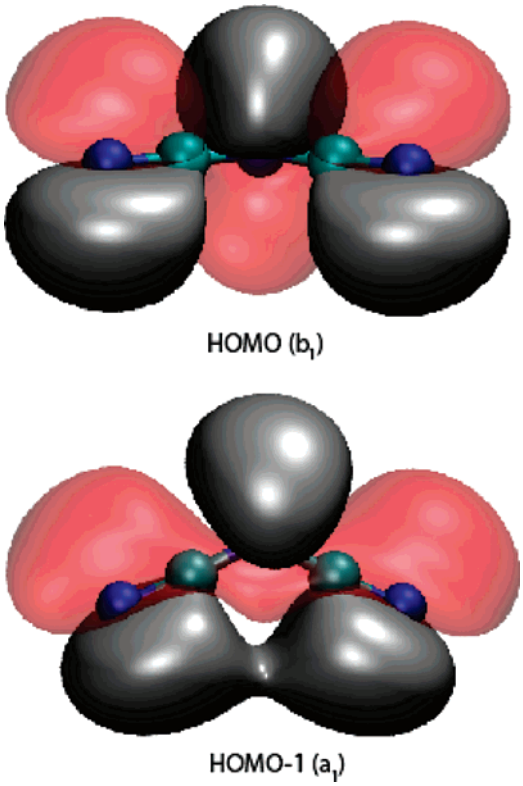

Figure 7. Frontier molecular orbitals of $N(CN)_2^-$.

of $n = 1-4$ and for the global minimum structures of $n = 5$ and 6 are presented in Table 1. The calculated VDEs for the global minimum structures at the MP2/aug-cc-pvdz level are for $n = 1-3$ in excellent (almost too good) agreement with the experimental data, as shown in Figure 2 (vertical bars) and in Figure 3. For $n = 4-6$ small deviations occur, but since they are within 0.2 eV they can be safely assigned to the anticipated inaccuracy of the MP2/aug-cc-pvdz level of theory.[33] The VDEs using the CCSD(T) method are slightly smaller than that from the MP2 calculations. The stepwise stabilization energy defined as $\Delta\mathrm{VDE}(n) = \mathrm{VDE}(n) - \mathrm{VDE}(n-1)$ (Figure 3b) is ~0.4 eV for the first two waters and decreases as n increases. The theoretical results show a similar trend (Figure 3). The observed incremental stabilization energies as a function of water suggest that the first five water molecules strongly interact with $N(CN)_2^-$, and additional waters provide much less stabilization to the charge of $N(CN)_2^-$. This observation is consistent with the theoretical structures (Figures 5 and 6) that the first four waters are directly bonded to the solute, whereas for $n = 5$ and 6 the additional waters begin to form a second solvation shell.

6. Conclusions

In summary, we report a synergetic experimental and theoretical study of $[N(CN)_2^-](H_2O)_n$ using PES and ab initio calculations. Vibrationally resolved PES spectra for the bare $N(CN)_2^-$ anion allow us to accurately measure the electron affinity of the $N(CN)_2$ radical as 4.135 ± 0.010 eV, as well as its bending and terminal C−N stretching frequencies. Detailed electronic and structural information about the microsolvation of the $N(CN)_2^-$ anion is obtained. The energetics and structures of the hydrated clusters are shown to be dictated by the subtle balance between the anion−water and water−water interactions. Starting with $n = 2$, the water−water H-bond becomes significant, and the second shell water molecules are observed to begin with $n = 5$ or 6. The unique three-hydration sites in the $N(CN)_2^-$ anion lead to a complex buildup of solvation shell.

Acknowledgment. The experimental work was supported by the U.S. Department of Energy (DOE), Office of Basic Energy Sciences, Chemical Sciences Division, and was performed at the EMSL, a national scientific user facility sponsored by DOE's Office of Biological and Environmental Research and located at Pacific Northwest National Laboratory, which is operated for DOE by Battelle. Support from the Czech Ministry of Education (Grants LC512 and ME644) and from the US NSF (Grants CHE-0431512 and CHE-0209719) for the theoretical work, and from the National Natural Science Foundation of China (Grant 20528303) is gratefully acknowledged.

References and Notes

(1) Burdick, W. L. *J. Am. Chem. Soc.* **1925**, *47*, 1485.
(2) Miller, J. S.; Manson, J. L. *Acc. Chem. Res.* **2001**, *34*, 563.
(3) Lotsch, B. V.; Senker, J.; Kockelmann, W.; Schnick, W. *J. Solid State Chem.* **2003**, *176*, 180.
(4) Jürgens, B.; Irran, E.; Schnick, W. *J. Solid State Chem.* **2001**, *157*, 241.
(5) Jürgens, B.; Höppe, H. A.; Schnick, W. *Solid State Sci.* **2002**, *4*, 821.
(6) Dressel, M.; Drichko, N.; Schlueter, J.; Bogdanova, O.; Zhilyaeva, E.; Lyubovskaya, R.; Greco, A.; Merino, J. *J. Phys. IV Fr.* **2004**, *114*, 475.
(7) Zhu, L.; Yao, K. L.; Liu, Z. L. *Chem. Phys. Lett.* **2006**, *424*, 209.
(8) Sprague, J. W.; Grasselli, J. G.; Ritchey, W. M. *J. Phys. Chem.* **1964**, *68*, 431.
(9) Frankel, M. B.; Burns, E. A.; Butler, J. C.; Wilson, E. R. *J. Org. Chem.* **1963**, *28*, 2428.
(10) Garbuz, S. V.; Skopenko, V. V.; Khav'ruchenko, V. D.; Gerasimchuk, N. N. *J. Theor. Exp. Chem.* **1989**, *25*, 92.
(11) Georgieva, M. K.; Binev, I. G. *J. Mol. Struct.* **2005**, *752*, 14.
(12) Pyykkö, P.; Runeberg, N. *J. Mol. Struct. (Theochem)* **1991**, *234*, 279.
(13) Christe, K. O.; Wilson, W. W.; Sheehy, J. A.; Boatz, J. A. *Angew. Chem., Int. Ed.* **1999**, *38*, 2004.
(14) Bernhardi, I.; Drews, T.; Seppelt, K. *Angew. Chem., Int. Ed.* **1999**, *38*, 2232.
(15) MacFarlane, D. R.; Golding, J.; Forsyth, S.; Forsyth, M.; Deacon, G. B. *Chem. Commun.* **2001**, 1430.
(16) Dahl, K.; Sando, G. M.; Fox, D. M.; Sutto, T. E.; Owrutsky, J. C. *J. Chem. Phys.* **2005**, *123*, 084504-1-11.
(17) Lopes, J. N. C.; Pádua, A. A. H. *J. Phys. Chem. B* **2006**, *110*, 19586.
(18) Wang, X. B.; Yang, X.; Wang, L. S. *Int. Rev. Phys. Chem.* **2002**, *21*, 473.
(19) Markovich, G.; Pollack, S.; Giniger, R.; Cheshnovsky, O. *J. Chem. Phys.* **1994**, *101*, 9344.
(20) Lehr, L.; Zanni, M. T.; Frischkorn, C.; Weinkauf, R.; Neumark, D. M. *Science* **1999**, *284*, 635.
(21) Yang, X.; Fu, Y. J.; Wang, X. B.; Slavíček, P.; Mucha, M.; Jungwirth, P.; Wang, L. S. *J. Am. Chem. Soc.* **2004**, *126*, 876.
(22) Minofar, B.; Mucha, M.; Jungwirth, P.; Yang, X.; Fu, Y. J.; Wang, X. B.; Wang, L. S. *J. Am. Chem. Soc.* **2004**, *126*, 11691.
(23) Wang, X. B.; Nicholas, J. B.; Wang, L. S. *J. Chem. Phys.* **2000**, *113*, 10837.
(24) Wang, X. B.; Yang, X.; Nicholas, J. B.; Wang, L. S. *Science* **2001**, *294*, 1322.
(25) Wang, X. B.; Woo, H. K.; Jagoda-Cwiklik, B.; Jungwirth, P.; Wang, L. S. *Phys. Chem. Chem. Phys.* **2006**, *8*, 4294.
(26) Wang, X. B.; Yang, X.; Wang, L. S.; Nicholas, J. B. *J. Chem. Phys.* **2002**, *116*, 561.
(27) Yang, X.; Kiran, B.; Wang, X. B.; Wang, L. S.; Mucha, M.; Jungwirth, P. *J. Phys. Chem. A* **2004**, *108*, 7820.
(28) Wang, L. S.; Ding, C. F.; Wang, X. B.; Barlow, S. E. *Rev. Sci. Instrum.* **1999**, *70*, 1957.
(29) Wang, X. B.; Woo, H. K.; Kiran, B.; Wang, L. S. *Angew. Chem., Int. Ed.* **2005**, *44*, 4968.
(30) Wang, X. B.; Woo, H. K.; Wang, L. S. *J. Chem. Phys.* **2005**, *123*, 051106.
(31) Frisch, M. J.; et al. *Gaussian 03*; Gaussian, Inc.: Pittsburgh, PA, 2003.
(32) Boys, S. F.; Bernardi, F. *Mol. Phys.* **1970**, *19*, 558.
(33) Young, D. *Computational Chemistry*; Wiley: New York, 2002.